

Hybrid Optimization for Enhanced Process Control in Fused Filament Fabrication of Carbon Fiber Reinforced Polyamide Composites

A. Abdullah, A. Iqbal, T. A. Shams, M. Ayaz, W. Tehami

¹College of Aeronautical Engineering, National University of Sciences and Technology (NUST), H-12, Islamabad, Pakistan

aabdullah.im01cae@student.nust.edu.pk

Abstract

Material characteristics play a significant role in the engineering design process. Enhancing these properties through improved processing techniques and tighter process control is essential for achieving optimal outcomes. Fiber-reinforced additive manufacturing (FRAM) enables the production of composite parts with high mechanical performance, with Fused Filament Fabrication (FFF) being the most common AM method using fibre-reinforced polymer filaments. Among these, carbon fibre reinforced polyamide (CF-PA) is of particular interest due to its favourable strength-to-weight ratio and thermal stability.

The properties of short carbon fibre reinforced polyamide composites are highly sensitive to variations in process parameters. In this study, initial optimization was carried out using a Taguchi Design of Experiments (DoE) approach, evaluating the influence of print speed (40–60 mm/s), print temperature (260–280 °C), layer height (0.25–0.35 mm), and raster angle (30–60°) on performance using an FFF-type 3D printer. However, Taguchi DoE, being a single-level optimization technique, cannot adequately capture the interaction effects between parameters.

To address this limitation, a hybrid optimization methodology was developed, using an objective function derived from the Taguchi analysis as a base for further refinement via genetic algorithms (GA). This approach demonstrates improved process control and enables the identification of optimal parameter combinations considering higher-order interactions.

The research provides a comparative analysis of traditional Taguchi DoE and the proposed hybrid optimization method, highlighting the improvements in both dimensional precision and porosity of carbon fibre reinforced polyamide structures. These findings offer meaningful insights into the FFF process and present a pathway toward more robust, cost-effective, and precise manufacturing of additively manufactured fibre-reinforced polymer (FRP) components.

3D printing, Hybrid optimization, Polymer, Property enhancement

1. Introduction

Fused Filament Fabrication (FFF) is a widely adopted additive manufacturing (AM) method for producing complex geometries at low cost and rapid turnaround [1][2][3]. The quality and performance of FFF-produced parts are governed by multiple process parameters [1], notable among them are nozzle temperature[4], print speed, layer height [5], and raster angle [6]. These parameters shape bead deposition, inter-layer fusion, and thermal history which have a significant impact on parts properties. Carbon fiber reinforced polyamide (CF-PA) is particularly attractive for high-performance applications owing to its favorable strength-to-weight ratio and thermal stability [1][3][7]. However, CF-PA parts are prone to defects such as dimensional precision loss (commonly evaluated via volumetric expansion) and porosity, both of which degrade mechanical performance and geometric fidelity [8]. These sensitivities underscore the need for effective process control strategies. Traditional Design of Experiments (DoE) methods, including full factorial and Taguchi designs, have proven useful for initial screening and robust factor selection [9][10]. Yet, Taguchi's single-level approach is limited in its ability to capture higher-order interactions among parameters [11][12][13]. To address this, we adopt a hybrid methodology: Taguchi L9 screening to establish robust baselines and response trends, followed by refinement using genetic algorithms (GA) driven by an objective function derived from regression of Taguchi results. The goal is

to improve process control with respect to dimensional precision (via volumetric expansion) and porosity for improving quality of printed parts. This study effectively utilized regression analysis on Taguchi experimental results, subsequently employing a genetic algorithm to achieve enhanced process control. This comprehensive approach ultimately aims to significantly improve the quality of fused filament fabricated parts.

2. Methodology

2.1. Materials and Equipment

Short carbon fiber reinforced PA6 (CF-PA6) filament (1.75 mm) was printed on an IEMA Magic HT Pro high-temperature FFF printer (enclosed chamber) with a 0.4 mm hardened nozzle. The chamber and bed were held at 90 °C and 120 °C, respectively. Cooling fans were off. Specimens were solid (100% infill) with a longitudinal infill pattern and printed in a constant orientation. Geometry followed ASTM D695 rectangular compression samples: 12.7 × 12.7 × 25.4 mm.

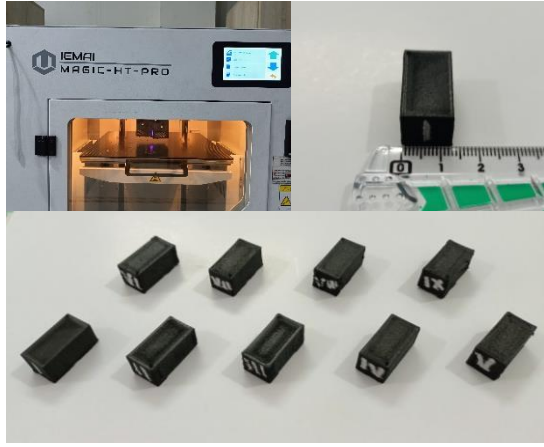


Figure 1. IEMA1 Magic HT Pro FFF Printer, ASTM D695 Samples

2.2. Taguchi Experimental Setup

A Taguchi L9 (3^4) orthogonal array was used to screen four factors at three levels: nozzle temperature (260, 270, 280 °C), print speed (40, 50, 60 mm/s), layer height (0.25, 0.30, 0.35 mm) and raster angle (30, 45, 60 deg). Factors and levels are mentioned in table-1. Fixed conditions during the process are listed in table-2. Measured responses were dimensional precision and part porosity.

Dimensional precision was quantified via volumetric expansion using Archimedes' method relative to the nominal CAD volume (4.096 cm³). Porosity (% area) was obtained from cross-sectional optical micrographs analyzed in ImageJ following standard thresholding and area-fraction computation. For Taguchi analysis, the "smaller-is-better" signal-to-noise (S/N) ratio definition was used for both outputs.

Table 1. Input factors and levels used in the Taguchi L9 design (baseline study)

Factor	Level 1	Level 2	Level 3
Print Temperature (°C)	260	270	280
Print Speed (mm/s)	40	50	60
Layer Height (mm)	0.25	0.30	0.35
Raster Angle (°)	30	45	60

Table 2. Invariable process parameters (baseline study)

Parameter	Value
Nozzle diameter	0.4 mm
Bed temperature	120 °C
Chamber temperature	90 °C
Infill density	100%
Infill pattern	Longitudinal
Cooling fan	Off

2.3. Hybrid Optimization

To overcome the inherent limitations of Taguchi analysis, which primarily focuses on main effects and predefined levels, a hybrid optimization approach was adopted to capture the complex, non-linear interactions prevalent in FFF processes [14][15]. This involved employing advanced regression modeling to accurately predict the two critical output responses: volumetric expansion and porosity. Specifically, linear regression was selected for modeling volumetric expansion due to its superior Leave-One-Out Cross-Validation (LOOCV) Mean Squared Error (MSE), while random forest regression proved most effective for predicting porosity, demonstrating its capability to capture more intricate relationships. Given the

small dataset size from the Taguchi L9 array, LOOCV was crucial for ensuring robust model evaluation and mitigating overfitting risks. Subsequently, a multi-objective genetic algorithm, NSGA-II, was utilized to leverage these predictive models. This allowed for a comprehensive exploration of the design space, enabling the identification of Pareto-optimal parameter sets that represent the best possible trade-offs between minimizing volumetric expansion and porosity, thereby providing a robust framework for informed process control.

3. Results and Discussion

This section integrates the baseline Taguchi results to establish a factual foundation that will be later compared with regression/GA-based optimization.

3.1. Taguchi Analysis

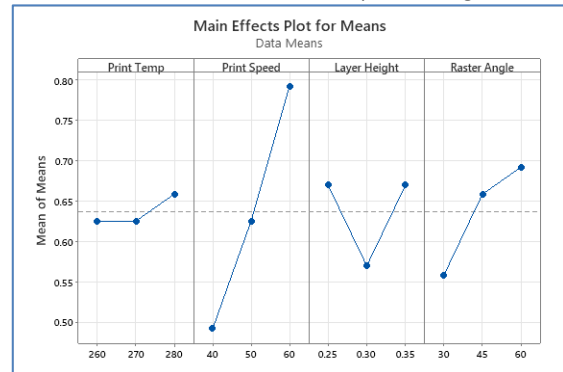
Table 3 reports the L9 matrix and measured responses from the baseline Taguchi analysis. Two output metrics were considered for analysis; dimensional precision and porosity. Volumetric expansion varied from 0.44-0.87 ml and porosity varied from 5.50-6.416%. Lowest expansion was observed at run-1 (260 °C, 40 mm/s, 0.25 mm, 30°) while minimum porosity was observed at run-6 (270 °C, 60 mm/s, 0.25 mm, 45°).

Table 3. Taguchi L9 experimental results (baseline study)

Run	Temp (°C)	Speed (mm/s)	Layer (mm)	Raster (°)	Vol. Exp. (ml)	Porosity (% area)	S/N (Vol. Exp.)	S/N (Porosity)
1	260	40	0.25	30	0.44	6.416	7.199	-16.145
2	260	50	0.30	45	0.57	6.092	4.884	-15.695
3	260	60	0.35	60	0.87	5.972	1.211	-15.522
4	270	40	0.30	60	0.47	6.132	6.560	-15.752
5	270	50	0.35	30	0.57	5.506	4.884	-14.817
6	270	60	0.25	45	0.84	5.359	1.550	-14.582
7	280	40	0.35	45	0.57	5.520	4.884	-14.839
8	280	50	0.25	60	0.74	6.155	2.656	-15.785
9	280	60	0.30	30	0.67	5.500	3.480	-14.807

3.1.1. Dimensional Precision (via volumetric expansion)

The lowest expansion (highest dimensional precision) was observed at Run 1 (260 °C, 40 mm/s, 0.25 mm, 30°) while the highest expansion was observed at Run 3 (260 °C, 60 mm/s, 0.35 mm, 60°). Print speed exerts the strongest adverse effect on dimensional precision: increasing speed from 40 to 60 mm/s increases expansion markedly. Layer height exhibits a non-monotonic trend, with 0.30 mm typically minimizing expansion versus 0.25/0.35 mm. Raster angle tends to worsen expansion as it increases (30° to 60°), consistent with bead alignment and thermal distortion effects. Temperature shows the mildest influence within 260–280 °C, with slightly better dimensional precision at the low end. Trends are depicted in figure-2.



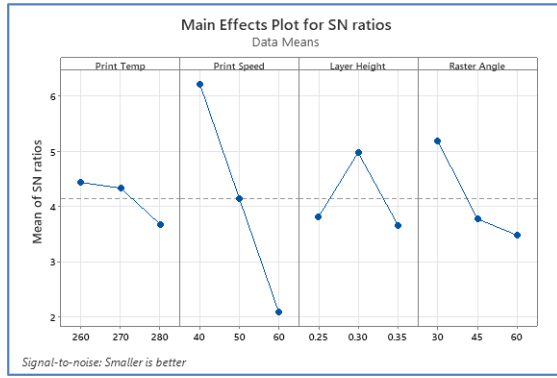


Figure 2. Main effects (means) and S/N ratio for dimensional precision (lower expansion is better)

3.1.2. Porosity Analysis

All the studied parameters exert significant influence on porosity of the printed parts. Print speed and layer height show monotonic trends with porosity decreasing with increasing levels but print temperature and raster angle show non-monotonic behavior with intermediate levels yielding better results. Print temperature (from 260 °C up to 270 °C), print speed and layer height improve porosity as they increase. Raster angle improves porosity up to 45° and then has adverse effect. Medium nozzle temperature (270 °C), high speed (60 mm/s), high layer height (0.35 mm) and medium raster angle (45°) are favorable for achieving low porosity in the printed parts. Trends are depicted in figure-3.

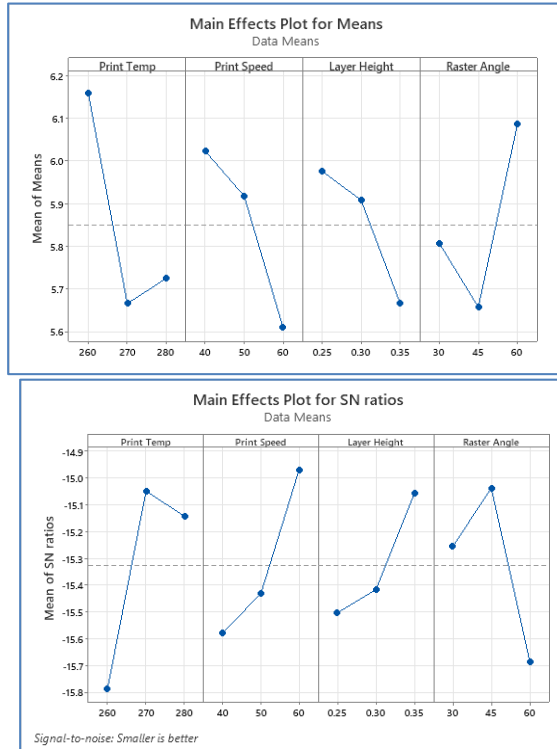


Figure 3. Main effects (means) and S/N ratio for porosity (smaller-is-better)

3.2. Regression Modeling

Taguchi model and analysis has an inherent limitation that it can only map process at the pre-defined set levels and can only give main effects [11]. However, FFF is very sensitive to input parameters, and their interaction effects play a key role in determining final properties of printed parts. Therefore, there is a need to employ further modeling methodologies for better process visibility [14]. To better understand the relationships between process parameters and the measured responses

(Volumetric Difference and Porosity), and to prepare for genetic algorithm-based optimization, multiple regression models were applied to the Taguchi L9 experimental data including **Linear Regression** (main effects only), **Polynomial Regression** (including 2-way interaction terms), and **Random Forest Regression**. Model performance was assessed using **R-squared**, **Adjusted R-squared** (for linear models), and **Cross-Validation Mean Squared Error (MSE)** via **Leave-One-Out Cross-Validation (LOOCV)**. LOOCV was chosen to ensure robust evaluation given the small dataset size. Linear regression model was used after comparison of model metrics for predicting volumetric difference as its **Cross-Validation (LOOCV) MSE** was lowest. Random Forest Regression was considered for predicting Porosity (% Area) due to its lowest CV MSE, suggesting it captures more complex non-linear relationships effectively.

With only 9 data points in the Taguchi L9 array, fitting complex models is challenging because of limited degrees of freedom. Overfitting is a significant risk, which is why LOOCV was used. LOOCV provides a realistic measure of predictive power on unseen data and is essential when working with small experimental datasets.

Table 4. Regression Models Comparison

Regression Model	Dimensional Precision	Porosity
	LOOCV MSE	
Linear Reg.	0.0157	0.2350
Polynomial Reg. (2 nd Ord)	0.0295 (over-fit)	2.4098 (over-fit)
Random Forest Reg.	0.0227	0.1471

3.3. GA Optimization

Following the regression analysis on the Taguchi L9 dataset, linear regression was identified as the most suitable model for predicting volumetric expansion, whereas random forest regression yielded the most accurate predictions for porosity. Due to the limited dataset size, a multi-objective genetic algorithm (NSGA-II) was employed to explore the trade-off between the two responses and identify Pareto-optimal parameter sets. The optimization results revealed multiple non-dominated solutions, where no single parameter combination simultaneously minimized both volumetric expansion and porosity. Among these, the parameter set corresponding to P1 achieved the lowest volumetric expansion, while P4 provided the minimum porosity value. The Pareto front (table 5) clearly illustrates the inherent trade-off between the two objectives, enabling informed selection of processing parameters based on specific performance priorities.

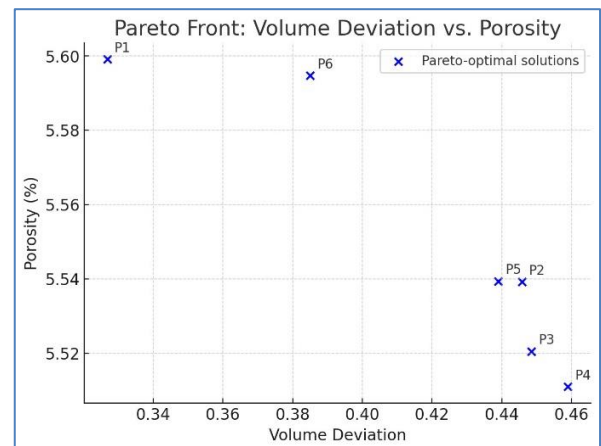


Figure 4. Pareto Optimal Solution Plots

Table 5. Pareto Optimal Solution Output Values

Pareto Front Point	Dimensional Precision (ml)	Porosity (%)
P1	0.3269	5.5991
P2	0.4457	5.5392
P3	0.4485	5.5205
P4	0.4589	5.5110
P5	0.4390	5.5394
P6	0.3850	5.5947

3.4. Trade-offs and Verification Baseline

The baseline study demonstrates clear trade-offs between dimensional precision and porosity. Parameter settings that minimize expansion (Run 1: 260 °C, 40 mm/s, 0.25 mm, 30°) exhibit the highest porosity (6.416%). Whereas the parameters which minimize porosity (Run 6: 270 °C, 60 mm/s, 0.25 mm, 45°) exhibit near-maximum expansion (0.84 ml), i.e., poor dimensional precision. Balanced settings emerge at Run 5 (270 °C, 50 mm/s, 0.35 mm, 30°) and Run 7 (280 °C, 40 mm/s, 0.35 mm, 45°), both showing moderate porosity (~5.51–5.52%) and lower expansion (0.57 ml). These observations motivate multi-objective optimization and directly justify our hybrid approach: Taguchi screening to establish baselines and rank sensitivities, followed by regression/GA to capture interactions and map the design space more effectively. Use of GA also depicts trade-offs between the two outputs but by mapping in the intermediate design space between the set Taguchi factor levels, it provides with better balance between both the outputs by further minimizing volumetric expansion while keeping porosity towards the lower bounds.

4. Conclusions and Future Work

This study successfully demonstrated a hybrid optimization methodology for Fused Filament Fabrication of carbon fiber reinforced polyamide composites, integrating Taguchi L9 screening with regression modeling and a multi-objective genetic algorithm (NSGA-II). Initial Taguchi analysis revealed the dominant influence of print speed and raster angle on dimensional precision, while all four parameters significantly impacted porosity, highlighting inherent trade-offs between these critical quality metrics. To overcome the limitations of Taguchi's single-level approach and capture complex parameter interactions, distinct regression models (linear for volumetric expansion and random forest for porosity) were developed and subsequently employed within the NSGA-II framework. The resulting Pareto optimal front clearly delineated the non-dominated solutions, providing a spectrum of parameter sets that balance volumetric expansion and porosity, enabling informed selection based on specific performance priorities. Future work will focus on the comprehensive integration of the full regression dataset, further refinement of the predictive models, and experimental validation of the GA-predicted optimal parameter sets to confirm their real-world efficacy.

References

- [1] K. Rithika and J. Sudha, "Additive Manufacturing of Fiber-Reinforced Composites—A Comprehensive Overview," Dec. 01, 2024, *John Wiley and Sons Ltd.* doi: 10.1002/pat.70002.
- [2] S. Yuan, S. Li, J. Zhu, and Y. Tang, "Additive manufacturing of polymeric composites from material processing to structural design," *Compos. Part B Eng.*, vol. 219, p. 108903, Aug. 2021, doi: 10.1016/j.compositesb.2021.108903.
- [3] N. van de Werken, H. Tekinalp, P. Khanbolouki, S. Ozcan, A. Williams, and M. Tehrani, "Additively manufactured carbon fiber-reinforced composites: State of the art and perspective," Jan. 01, 2020, *Elsevier B.V.* doi: 10.1016/j.addma.2019.100962.
- [4] A. Pulipaka, K. Gide, A. Beheshti, and Z. Bagheri, "Effect of 3D printing process parameters on surface and mechanical properties of FFF-printed PEEK," *J. Manuf. Process.*, 2023, doi: 10.1016/j.jmapro.2022.11.057.
- [5] K. M. Agarwal, P. Shubham, D. Bhatia, P. Sharma, H. Vaid, and R. Vajpeyi, "Analyzing the Impact of Print Parameters on Dimensional Variation of ABS specimens printed using Fused Deposition Modelling (FDM)," *Sensors Int.*, vol. 3, p. 100149, 2022, doi: 10.1016/j.sintl.2021.100149.
- [6] S. Srinivasan Ganesh Iyer and O. Keles, "Effect of raster angle on mechanical properties of 3D printed short carbon fiber reinforced acrylonitrile butadiene styrene," *Compos. Commun.*, vol. 32, p. 101163, Jun. 2022, doi: 10.1016/j.coco.2022.101163.
- [7] B. Brenken, E. Barocio, A. Favaloro, V. Kunc, and R. B. Pipes, "Fused filament fabrication of fiber-reinforced polymers: A review," *Addit. Manuf.*, vol. 21, pp. 1–16, May 2018, doi: 10.1016/j.addma.2018.01.002.
- [8] S. Wickramasinghe, T. Do, and P. Tran, "FDM-Based 3D Printing of Polymer and Associated Composite: A Review on Mechanical Properties, Defects and Treatments," *Polymers (Basel)*, vol. 12, no. 7, p. 1529, Jul. 2020, doi: 10.3390/polym12071529.
- [9] S. Chen, L. Cai, Y. Duan, X. Jing, C. Zhang, and F. Xie, "Performance enhancement of <sc>3D</sc>-printed carbon fiber-reinforced nylon 6 composites," *Polym. Compos.*, vol. 45, no. 6, pp. 5754–5772, Apr. 2024, doi: 10.1002/pc.28161.
- [10] J. Wong, A. Altassan, and D. W. Rosen, "Additive manufacturing of fiber-reinforced polymer composites: A technical review and status of design methodologies," *Compos. Part B Eng.*, vol. 255, p. 110603, Apr. 2023, doi: 10.1016/j.compositesb.2023.110603.
- [11] B. Beylergil, A. Al-Nadhari, and M. Yildiz, "Optimization of Charpy-impact strength of <sc>3D</sc>-printed carbon fiber/polyamide composites by Taguchi method," *Polym. Compos.*, vol. 44, no. 5, pp. 2846–2859, May 2023, doi: 10.1002/pc.27285.
- [12] G. Taguchi, *Introduction to quality engineering: designing quality into products and processes*. 1986.
- [13] A. Mitra, "The Taguchi method," *Wiley Interdiscip. Rev. Comput. Stat.*, vol. 3, 2011, doi: 10.1002/wics.169.
- [14] K. Stergiou, C. Ntakolia, P. Varytis, E. Koumoulos, P. Karlsson, and S. Moustakidis, "Enhancing property prediction and process optimization in building materials through machine learning: A review," *Comput. Mater. Sci.*, vol. 220, p. 112031, Mar. 2023, doi: 10.1016/j.commatsci.2023.112031.
- [15] P. Charalampous, N. Kladovasilakis, I. Kostavelis, K. Tsongas, D. Tzetzis, and D. Tzovaras, "Machine Learning-Based Mechanical Behavior Optimization of 3D Print Constructs Manufactured Via the FFF Process," *J. Mater. Eng. Perform.*, vol. 31, no. 6, pp. 4697–4706, Jun. 2022, doi: 10.1007/s11665-021-06535-0.